LETTER

doi:10.1038/nature11206

Genetic dissection of the circuit for hand dexterity in primates

Masaharu Kinoshita[1], Ryosuke Matsui[2], Shigeki Kato[3], Taku Hasegawa[2], Hironori Kasahara[2], Kaoru Isa[1], Akiya Watakabe[4,5], Tetsuo Yamamori[4,5], Yukio Nishimura[1,5,6], Bror Alstermark[7], Dai Watanabe[2], Kazuto Kobayashi[3] & Tadashi Isa[1,5]

It is generally accepted that the direct connection from the motor cortex to spinal motor neurons is responsible for dexterous hand movements in primates[1–3]. However, the role of the 'phylogenetically older' indirect pathways from the motor cortex to motor neurons, mediated by spinal interneurons, remains elusive. Here we used a novel double-infection technique to interrupt the transmission through the propriospinal neurons (PNs)[4–6], which act as a relay of the indirect pathway in macaque monkeys (*Macaca fuscata* and *Macaca mulatta*). The PNs were double infected by injection of a highly efficient retrograde gene-transfer vector into their target area and subsequent injection of adeno-associated viral vector at the location of cell somata. This method enabled reversible expression of green fluorescent protein (GFP)-tagged tetanus neurotoxin, thereby permitting the selective and temporal blockade of the motor cortex–PN–motor neuron pathway. This treatment impaired reach and grasp movements, revealing a critical role for the PN-mediated pathway in the control of hand dexterity. Anti-GFP immunohistochemistry visualized the cell bodies and axonal trajectories of the blocked PNs, which confirmed their anatomical connection to motor neurons. This pathway-selective and reversible technique for blocking neural transmission does not depend on cell-specific promoters or transgenic techniques, and is a new and powerful tool for functional dissection in system-level neuroscience studies.

Lesion studies at the level of the brainstem[1] in macaque monkeys showed that the performance of highly fractionated finger movements primarily depends on the pyramidal tract. Later studies proposed that the direct corticomotoneuronal connection (the monosynaptic connection from cortical neurons to motor neurons)[2,3], which is unique to higher primates, is the basis for dexterous hand movements. In less dexterous animals such as cats, the corticospinal tract (CST) is not directly connected to hand–arm motor neurons. In these animals, the shortest pathway from the cortex to motor neurons is disynaptic, mainly involving spinal interneurons located either in the same segments as motor neurons (caudal to C6; segmental interneurons) or in more rostral segments (mainly in C3–C5; PNs)[4]. Evidence that the non-monosynaptic pathway is conserved in monkeys was provided recently[5,6]. Contribution of this phylogenetically older PN-mediated pathway has been assessed in behavioural experiments that determined the effects of specific lesions of the CST at the C5 and C2 segments, thereby leaving the PN axons intact[7–10]. The results indicated that the PN-mediated pathway could control independent finger movements. However, because the lesions were irreversible, it is possible to consider that the indirect pathway was responsible for the recovery of function, rather than contributing to hand dexterity in the intact state[3]. This problem could be solved if it is possible to block the PNs specifically and temporarily. For this purpose, we combined two viral vectors for the selective and reversible blockade of the PN-mediated pathway (Fig. 1); first, the highly efficient retrograde gene transfer (HiRet) lentiviral vector[11] carrying enhanced tetanus neurotoxin light chain (eTeNT)[12] (Supplementary Fig. 1) and the enhanced GFP (EGFP) downstream of the tetracycline-responsive element (TRE)[13]; and second, the adeno-associated virus serotype 2 (AAV2) vector carrying the Tet-on sequence, a variant of reverse tetracycline transactivator (rtTAV16)[14] (see Methods) under the control of the cytomegalovirus (CMV) promoter.

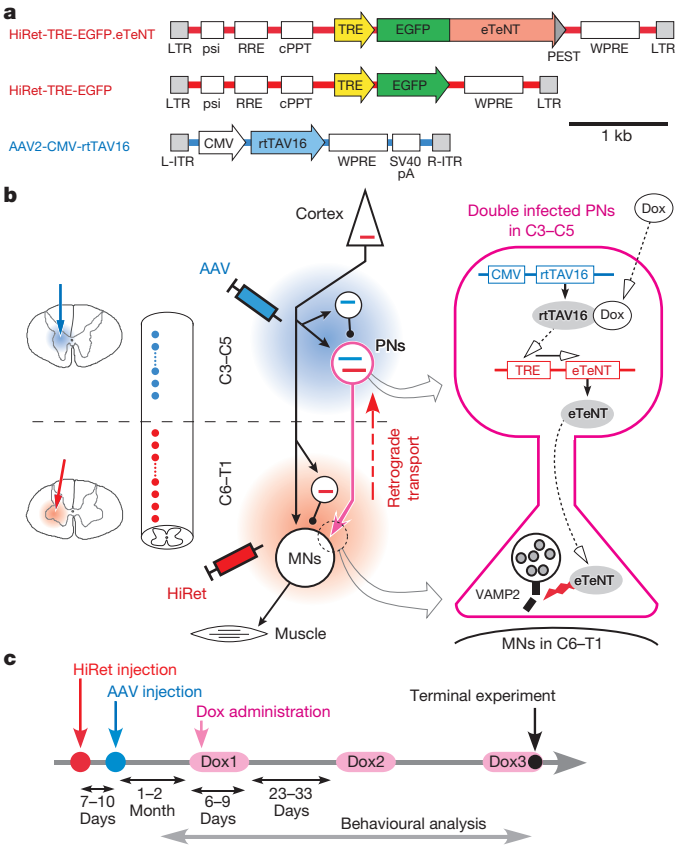

Figure 1 | The pathway-specific and reversible blockade of synaptic transmission. **a**, The design of viral vectors. **b**, Schematic diagrams of vector injections and how HiRet-TRE-EGFP.eTeNT and AAV2-CMV-rtTAV16 interact in the double-infected cells. **c**, The experimental schedule. cPPT, central polypurine tract; Dox, doxycycline; L- and R-ITR, left and right inverted terminal repeat; LTR, long terminal repeat; MNs, motor neurons; RRE, Rev responsive element; PEST, PEST sequence; psi, packaging signal; VAMP2, vesicle-associated membrane protein 2 sequence; WPRE, Woodchuck hepatitis virus post-transcriptional regulatory element.

[1]Department of Developmental Physiology, National Institute for Physiological Sciences, Myodaiji, Okazaki 444-8585, Japan. [2]Department of Molecular and System Biology, Graduate School of Biostudies, Kyoto University, Sakyo-ku, Kyoto 606-8501, Japan. [3]Department of Molecular Genetics, Institute of Biomedical Sciences, Fukushima Medical University School of Medicine, Fukushima 960-1295, Japan. [4]Division of Brain Biology, National Institute for Basic Biology, Okazaki 444-8585, Japan. [5]The Graduate University for Advanced Studies (Sokendai), Hayama, Kanagawa 240-0193, Japan. [6]Precursory Research for Embryonic Science and Technology (PRESTO), Japan Science and Technology Agency (JST), Chiyoda, Tokyo 102-0076, Japan. [7]Department of Integrative Medical Biology, section of Physiology, Umeå University, S-901 87 Umeå, Sweden.

HiRet-TRE-EGFP.eTeNT was injected into the region containing motor neurons targeted by the PNs (that is, the ventral horn of the C6–T1 segments (T1 is the first thoracic segment)), and AAV2-CMV-rtTAV16 was injected 7 to 10 days later, into the intermediate zone of the caudal C2 to rostral C5 segments where their cell bodies are located (Supplementary Table 1). Thus, PNs with cell bodies in the mid-cervical segments and with axons that contact the hand–arm motor neurons would be double infected. During administration of doxycycline, expression of eTeNT depresses synaptic transmission in the PNs selectively and spares other inputs to the motor neurons.

We tested four monkeys (H, K, B and N) with double injection of HiRet-TRE-EGFP.eTeNT and AAV2-CMV-rtTAV16, and one additional monkey (S) was injected with HiRet-TRE-EGFP, which lacks the eTeNT of HiRet-TRE-EGFP.eTeNT (Fig. 1a), and used as a control.

One to two months after the injections, the oral administration of doxycycline was initiated to induce the expression of eTeNT. Two to five days after beginning administration, all four monkeys transfected with the eTeNT gene had profound deficits in reach and grasp movements. Typically, their movements were slowed with increased errors in precision grip and/or reach (Fig. 2e). Monkeys H and N showed deficits mainly in precision grip, in which thumb extension was particularly problematic (Fig. 2a, b and Supplementary Movies 1 and 4). Conversely, monkeys B and K had deficits in reach; their hands often hit the edge of the apparatus before reaching the food piece (Fig. 2c, d, and Supplementary Movies 2, 3 and 5). Hand movements in the control animal, monkey S, were not affected.

Despite the continued administration of doxycycline, impairment of the reach and grasp movements resolved over a period of 2 to 3 days. On day 6 to 8 of doxycycline administration, when the behavioural deficits disappeared, the blood concentration of doxycycline remained high (Supplementary Fig. 2) and transmission through the PNs was still largely blocked as revealed by electrophysiological experiments (see below; Fig. 3). These results indicated that the expression of eTeNT did not abate during doxycycline administration. Taken together, the results show that intact neural systems, including the direct corticomotoneuronal pathway or other indirect pathways (see the circuit diagram in Fig. 3a), would have compensated for the loss of control by the blocked PNs. When doxycycline administration was terminated and re-started 3 to 4 weeks later, all animals again showed deficits in reach and grasp movements. This indicates that the compensation by other pathways was only temporary and that the PNs recovered their control during the doxycycline-off period.

After behavioural testing was completed, electrophysiological experiments were performed to confirm the blockade of synaptic transmission through PNs in monkeys B, N and S. Stimulation of the contralateral medullary pyramid at 200 μA induced monosynaptic excitatory postsynaptic potentials (EPSPs) in motor neurons on both sides of the spinal cord (Supplementary Fig. 3b). The amplitudes of the evoked monosynaptic field potentials in the deep radial motor nucleus were not significantly different between the two sides (Fig. 3b, one-tailed t-test; $P = 0.34$ and 0.71, in monkeys B and N, respectively). These data indicate that the vectors did not adversely affect the direct corticomotoneuronal pathway. Indirect input to motor neurons mediated by the PNs was assessed by recording the disynaptic negative field potentials in the deep radial motor nucleus, which had segmental latencies in the range of 0.9–1.9 ms. This component remained after CST lesioning at the C5 level, but was almost completely abolished after C2 lesioning (Fig. 3c, d and Supplementary Fig. 4). This indicates

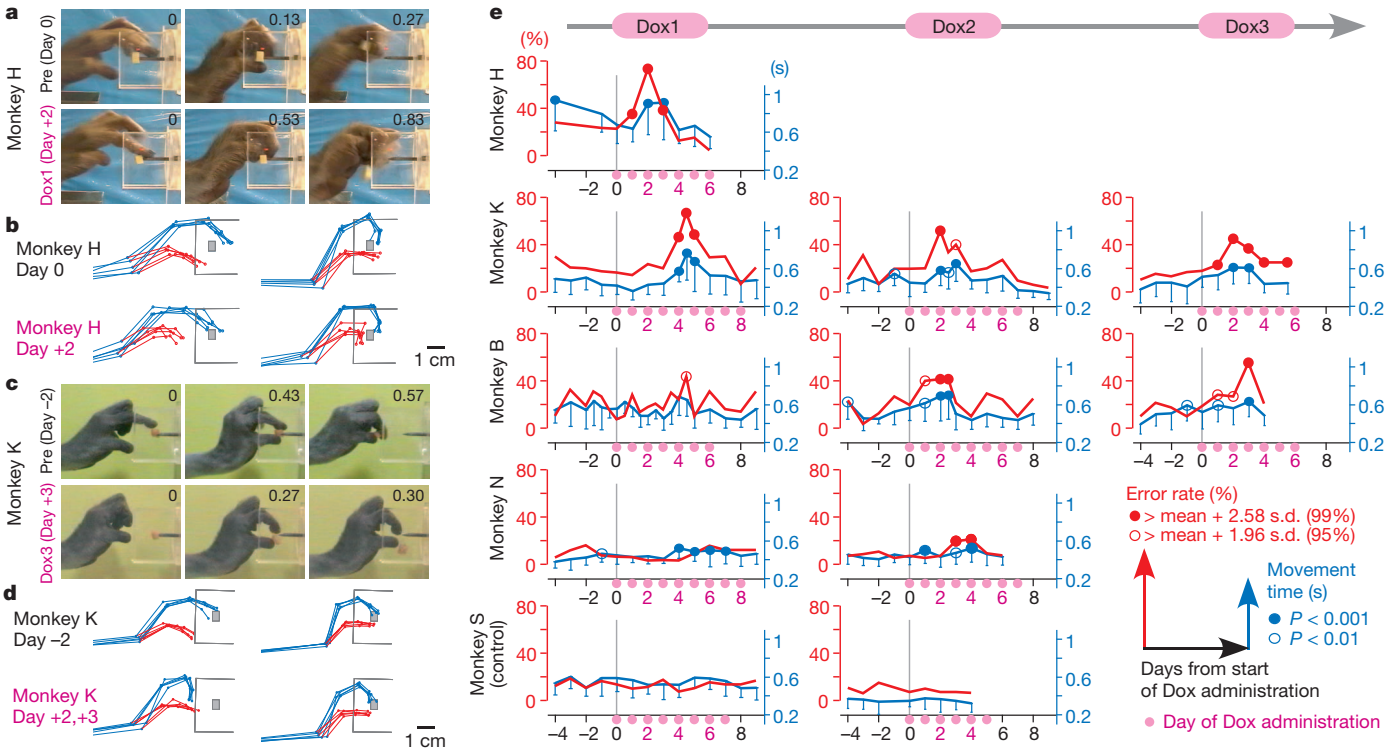

Figure 2 | Reversible impairment of reach and grasp movements during doxycycline administration. **a**–**d**, An example of reach and grasp movements before (Pre) and 2 days after doxycycline administration in monkey H (**a**). The monkey showed 'precision grip error' (Supplementary Movie 1). The first frame shows the initial contact of the index finger with the food piece and the second frame shows the first contact of the thumb with the food. The time from the first frame (in s) is indicated in each panel. Stick diagrams of reach and grasp movements of monkey H are shown in **b**. The index finger and wrist joint are shown in blue and the thumb in red, and five trials are superimposed. Reach and grasp movement before and 3 days after the doxycycline administration in monkey K, 'slit-hit error' (**c**) (Supplementary Movie 2). Stick diagrams of reach and grasp movements of monkey H are shown in **d**. Five trials are superimposed, and colours are as in **b**. The left panels of **b** and **d** correspond to the timing of the first frame in **a** and **c**, respectively. The right panels correspond to the second frame in **a** and **c**, respectively. **e**, Movement time (blue) and error rate (red) before and during doxycycline administration in all monkeys. The means (thick lines) and s.d. (thin vertical lines) of 30–100 trials are shown.

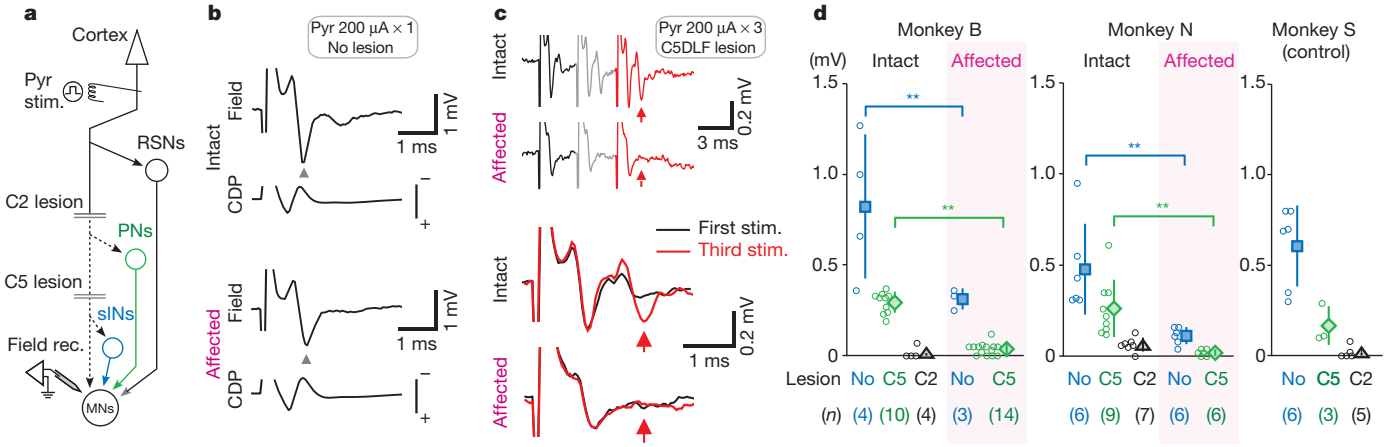

Figure 3 | Blockade of synaptic transmission through the PNs. **a**, The experimental arrangement. In addition to the direct corticomotoneuronal connection, there could be three possible routes of indirect pathways; through reticulospinal neurons (RSNs), PNs and segmental interneurons (sINs). During the experiments, the dorsolateral funiculus (DLF) was transected successively at the C5 and C2 levels (Supplementary Methods). Dashed lines, transected axons. Pyr, contralateral medullary pyramid. Arrowheads, presynaptic terminals. **b**, Monosynaptic field potentials (grey arrowheads) in the deep radial motor nucleus (top panel), and cord dorsum potential (CDP; bottom panel) on the intact and affected sides. **c**, Disynaptic field potentials evoked by triple stimulation of the contralateral medullary pyramid at 200 μA. Full records (top panel) and superimposed records of the expanded view of the responses following the first and third stimuli (bottom panel). **d**, Quantitative analysis of the disynaptic field potentials with no lesion, after CST lesioning at C5 and C2 in monkeys B, N and S. Means and s.d. values are also shown. *P* values showing a statistical difference are marked with asterisks (**, $P < 0.01$). The number of records are shown below.

that the field potential observed after C5 lesioning was mostly mediated by the PNs. On the affected sides of monkeys B and N, the disynaptic field potential became much smaller after the C5 lesioning (13% in monkey B and 6.8% in monkey N) compared to the intact side (Fig. 3c, d). In contrast, the disynaptic field potential on the injected side of the sham control (monkey S) showed similar amplitudes to the intact side of the other animals (Fig. 3d). These results confirmed that neural transmission by the majority of PNs (90%) had been blocked on the affected side. Corroborating results were observed from intracellular recordings in motor neurons (Supplementary Fig. 3). Finally, stimulation of the lateral reticular nucleus (LRN) in the brainstem induces the monosynaptic excitation of motor neurons that is mediated by axon reflex of the PNs[6,15] (Supplementary Fig. 5a). The results of LRN stimulation also indicated that the PN-mediated transmission was severely affected (Supplementary Figs 5b, c and 6).

Because EGFP was tagged to eTeNT, the additional expression of EGFP provided neuroanatomical confirmation that the neurons affected by eTeNT were PNs (Fig. 4a). Neurons marked with anti-GFP immunohistochemistry were concentrated in the lateral part of lamina VII and partly in laminae V, VI and VIII (Fig. 4b, c, e and Supplementary Fig. 7). This fits well with the location of previously reported PNs in cats[16,17] and monkeys[6]. *In situ* hybridization for the tTA sequence revealed that the AAV vector had infected many neurons in a wide area of the grey matter on the injected side (Fig. 4d, f). The GFP-positive cells comprised 1–2% of AAV2-CMV-rtTAV16-infected cells (Supplementary Table 2). They were most abundant in the C4 to rostral C5 segments and decreased in number at the C3 segment (Fig. 4f). Again, this distribution fits well with the distribution of the PNs reported in cats[17]. The total number of GFP-positive cells in monkeys K, B, N and S was in the range of 865–2,760. This number was smaller ($n = 294$) in monkey H, presumably reflecting its relatively short survival time (Supplementary Table 2). Interestingly, anti-GFP immunohistochemistry labelled not only the PN cell bodies but also their axons, particularly in monkeys N and S. In these animals, labelled axons were traced to the motor nuclei in the C6–T1 segments

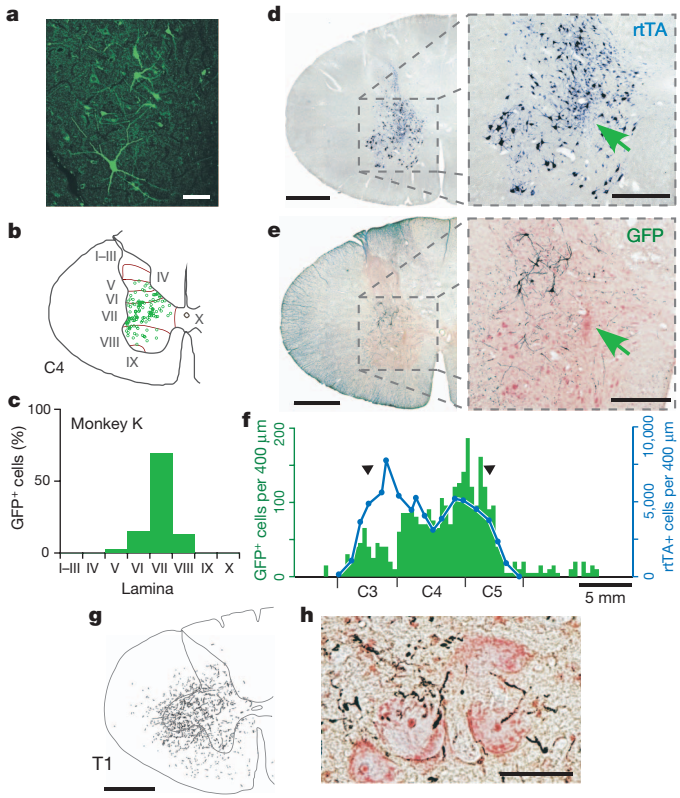

Figure 4 | Visualization of the blocked PNs. **a**, An example of GFP-positive cells. Scale bar, 100 μm. **b**, **c**, Distribution of GFP-positive cells in the C4 segment of monkey K (**b**) and their numbers in individual layers of Rexed (**c**). I–X, laminae. **d**, **e**, *In situ* hybridization and anti-GFP immunohistochemistry of the C4 segment of monkey K, which shows the AAV2-CMV-rtTAV16-infected neurons in dark blue (**d**) and GFP-positive cells shown in black by anti-GFP immunohistochemistry in an adjacent section counterstained with Neutral Red (**e**). Arrows, centre of the injection site. Left panel, scale bars are 1 mm. Right panel, scale bars are 500 μm. **f**, Longitudinal distribution of the GFP-positive cells (green columns). Blue lines show the distribution of the rtTA-positive cells. Black arrowheads, the rostral and caudal ends of the AAV2-CMV-rtTAV16 injections. **g**, Camera lucida drawings of GFP-positive axons and terminals at the level of the motor nucleus at the T1 segment in monkey N. Scale bar, 1 mm. **h**, Photomicrographs of axons and terminals (black) in the motor nucleus. The sections were counterstained with Neutral Red. Scale bar, 50 μm.

(Fig. 4g, h) and in the LRN (Supplementary Fig. 8b, c) showing that the injected vectors were effectively directed to the PNs.

Thus, we have succeeded in the pathway-selective and reversible blockade of synaptic transmission in primates by using double infection of viral vectors. Blockade of synaptic transmission through the PNs caused substantial, albeit temporary disruption of hand reach and of grasp dexterity. It has been proposed previously that a major advantage of the direct corticomotoneuronal connection for the control of independent finger movements is that the direct corticomotoneuronal connection bypasses these spinal interneurons, which were considered to have too widespread connections with motor neurons to control the fractionated finger movements[2]. However, our results indicate strongly that the PN-mediated indirect pathway is required for the control of hand dexterity in the intact state. The current technique is a notable extension of the permanent pathway-selective lesioning of the thalamostriatal pathway in mice reported recently[18]. This method can be used as a powerful tool for functional dissection of specific central pathways whose cell-specific promoters[12,19] are not known. This is particularly important in species such as primates, for which making transgenic animals is more difficult (compared with mice, for example) and for which no successful example of behavioural modification with optogenetics has been reported[20–22].

METHODS SUMMARY

Five macaque monkeys were used in the present study. The experimental protocols followed the principles of the National Institutes of Health, and the Ministry of Education, Culture, Sports, Science and Technology of Japan, and were approved by the Institutional Animal Care and Use Committee of the National Institutes of Natural Sciences, Japan. The monkeys were trained to perform reach and grasp movements in their home cage. Under anaesthesia, HiRet-TRE-EGFP.eTeNT was injected into the ventral horn of the C6–T1 spinal segments (16–19 tracks at 1-mm intervals, 0.5 μl vector solution in each track) in four monkeys (H, K, B and N). In one monkey (S), HiRet-TRE-EGFP was injected as a control. Seven to ten days later, the AAV2 vector carrying the rtTAV16 sequence was injected into the intermediate zone of the C2–C5 segments (8–13 tracks at 1-mm intervals, 0.5 μl vector solution in each track). One to two months later, the oral administration of doxycycline was initiated and continued for 6 to 9 days. Doxycycline administration was repeated for up to 3 times at 3- to 4-week intervals. Reach and grasp movements were tested before, during and after each administration period. On the last day of administration, electrophysiological experiments to evaluate transmission through the PNs were performed under anaesthesia and artificial ventilation. Under deep anaesthesia with sodium pentobarbital (50–100 mg kg^{-1}), all the monkeys were transcardially perfused and histological examinations were performed to visualize the blocked PNs using anti-GFP immunohistochemistry, and the AAV-infected cells were assessed using *in situ* hybridization for rtTA.

Full Methods and any associated references are available in the online version of the paper at www.nature.com/nature.

Received 14 December 2011; accepted 1 May 2012.
Published online 17 June 2012.

1. Lawrence, D. G. & Kuypers, H. G. The functional organization of the motor system in the monkey. I. The effect of bilateral pyramidal lesions. *Brain* **91,** 1–14 (1968).
2. Kuypers, H. G. A new look at the organization of the motor system. *Prog. Brain Res.* **57,** 381–403 (1982).
3. Lemon, R. N. Descending pathways in motor control. *Annu. Rev. Neurosci.* **31,** 195–218 (2008).
4. Alstermark, B. & Lundberg, A. in *Muscle Afferents and Spinal Control of Movement* (eds Jami, L., Pierrot-Deseilligny, E. & Zytnicki, D.) 327–354 (Pergamon Press, 1992).
5. Alstermark, B., Isa, T., Ohki, Y. & Saito, Y. Disynaptic pyramidal excitation in forelimb motoneurons mediated via C3–C4 propriospinal neurons in the Macaca fuscata. *J. Neurophysiol.* **82,** 3580–3585 (1999).
6. Isa, T., Ohki, Y., Seki, K. & Alstermark, B. Properties of propriospinal neurons in the C3–C4 segments mediating disynaptic pyramidal excitation to forelimb motoneurons in the macaque monkey. *J. Neurophysiol.* **95,** 3674–3685 (2006).
7. Sasaki, S. *et al.* Dexterous finger movements in primate without monosynaptic corticomotoneuronal excitation. *J. Neurophysiol.* **92,** 3142–3147 (2004).
8. Nishimura, Y. *et al.* Time-dependent central compensatory mechanisms of finger dexterity after spinal cord injury. *Science* **318,** 1150–1155 (2007).
9. Nishimura, Y., Morichika, Y. & Isa, T. A subcortical oscillatory network contributes to recovery of hand dexterity after spinal cord injury. *Brain* **132,** 709–721 (2009).
10. Alstermark, B. *et al.* Motor command for precision grip in the macaque monkey can be mediated by spinal interneurons. *J. Neurophysiol.* **106,** 122–126 (2011).
11. Kato, S. *et al.* A lentiviral strategy for highly efficient retrograde gene transfer by pseudotyping with fusion envelope glycoprotein. *Hum. Gene Ther.* **22,** 197–206 (2011).
12. Yamamoto, M. *et al.* Reversible suppression of glutamatergic neurotransmission of cerebellar granule cells *in vivo* by genetically manipulated expression of tetanus neurotoxin light chain. *J. Neurosci.* **23,** 6759–6767 (2003).
13. Gossen, M. & Bujard, H. Tight control of gene expression in mammalian cells by tetracycline-responsive promoters. *Proc. Natl Acad. Sci. USA* **89,** 5547–5551 (1992).
14. Zhou, X., Vink, M., Klaver, B., Berkhout, B. & Das, A. T. Optimization of the Tet-On system for regulated gene expression through viral evolution. *Gene Ther.* **13,** 1382–1390 (2006).
15. Alstermark, B., Lindström, S., Lundberg, A. & Sybirska, E. Integration in descending motor pathways controlling the forelimb in the cat. 8. Ascending projection to the lateral reticular nucleus from C3–C4 propriospinal also projecting to forelimb motoneurones. *Exp. Brain Res.* **42,** 282–298 (1981).
16. Illert, M., Lundberg, A. & Tanaka, R. Integration in descending motor pathways controlling the forelimb in the cat. 3. Convergence on propriospinal neurones transmitting disynaptic excitation from the corticospinal tract and other descending tracts. *Exp. Brain Res.* **29,** 323–346 (1977).
17. Alstermark, B. & Kümmel, H. Transneuronal transport of wheat germ agglutinin conjugated horseradish peroxidase into last order spinal interneurones projecting to acromio- and spinodeltoideus motoneurones in the cat. 1. Location of labelled interneurones and influence of synaptic activity on the transneuronal transport. *Exp. Brain Res.* **80,** 83–95 (1990).
18. Kato, S. *et al.* Selective neural pathway targeting reveals key roles of thalamostriatal projection in the control of visual discrimination. *J. Neurosci.* **31,** 17169–17179 (2011).
19. Yu, C. R. *et al.* Spontaneous neural activity is required for the establishment and maintenance of the olfactory sensory map. *Neuron* **42,** 553–566 (2004).
20. Yizhar, O., Fenno, L. E., Davidson, T. J., Mogri, M. & Deisseroth, K. Optogenetics in neural systems. *Neuron* **71,** 9–34 (2011).
21. Han, X. *et al.* A high-light sensitivity optical neural silencer: development and application to optogenetic control of non-human primate cortex. *Front. Syst. Neurosci.* **5,** 18 (2011).
22. Diester, I. *et al.* An optogenetic toolbox designed for primates. *Nature Neurosci.* **14,** 387–397 (2011).

Supplementary Information is linked to the online version of the paper at www.nature.com/nature.

Acknowledgements We thank S. Nakanishi, H. Jingami and C. Akazawa for continuous encouragement. We thank P. Redgrave for comments on the earlier version of the manuscript. This study was supported by the Strategic Research Program for Brain Sciences by the Ministry of Education, Culture, Sports, Science and Technology (MEXT) of Japan. B.A. was supported by the Swedish Research Council. We thank T. Oishi for providing macaque brain sample tissue. We thank P. Phongphanphanee, M. Togawa, Y. Yamanishi, T. Katoh, K. Shimizu, N. Takahashi and K. Takada for technical support.

Author Contributions M.K., D.W., K.K., B.A. and T.I. designed the experiments and wrote the paper. M.K., B.A., K.I. and T.I. conducted the surgery, behavioural, electrophysiological and histological experiments and analysed the data. R.M., T.H., S.K., H.K., D.W. and K.K. made the viral vectors. A.W. and T.Y. contributed to the histological processing. Y.N. contributed to behavioural analysis and electrophysiological experiments.

Author Information Reprints and permissions information is available at www.nature.com/reprints. The authors declare no competing financial interests. Readers are welcome to comment on the online version of this article at www.nature.com/nature. Correspondence and requests for materials should be addressed to T.I. (tisa@nips.ac.jp).

METHODS

Five macaque monkeys (three *Macaca fuscata* and two *Macaca mulatta*, body weight 3.1–6.0 kg) were used in the present study. The experimental protocols followed the guideline of the National Institutes of Health, and the Ministry of Education, Culture, Sports, Science and Technology (MEXT) of Japan, and were approved by the Institutional Animal Care and Use Committee of National Institutes of Natural Sciences. The time course of the experiments on individual animals is shown in Fig. 1c and Supplementary Table 1.

Immunoblot analysis. The soluble NSF attachment protein receptor (SNARE) cDNAs (*VAMP2*, *SNAP25* and *SNAP23*) were cloned from a macaque brain (*Macaca fuscata*) and subcloned into pCI (Promega) with an amino-terminal Flag-tag sequence (to generate pVAMP2, pSNAP25 and pSNAP23, respectively). Expression plasmids of wild-type TeNT and codon-optimized modified TeNTs (eTeNT and EGFP.eTeNT.PEST) contained the CMV. For Tet-on inducible expression of eTeNT, an rtTA2 expression plasmid containing the CMV (prtTA2) and pLV-TRE-EGFP.eTeNT.PEST was used. Forty-eight hours after transfection, the cells were collected. Immunoblots were performed using a mouse anti-Flag M2 monoclonal antibody (F1804, Sigma-Aldrich) and visualized with a horseradish peroxidase-conjugated sheep anti-mouse immunoglobulin-G (IgG) antibody (NA931V, GE Healthcare) (Supplementary Fig. 1).

Vector preparation. The highly efficient retrograde gene transfer (HiRet) vector is a pseudotype of a human immunodeficiency-virus-type-1-based lentiviral vector with fusion glycoprotein B type, which is composed of the extracellular and transmembrane domains of rabies virus glycoprotein and the cytoplasmic domain of vesicular stomatitis virus glycoprotein[11,18]. In the present study, the envelope plasmid encoding fusion glycoprotein B2 type under the control of the cytomegalovirus enhancer and chicken β-actin promoter[18] was used for vector production. Chimaeric EGFP.eTeNT.PEST was generated by fusing the human codon-optimized eTeNT with the EGFP cDNA of the pEGFP-N1 vector (Clontech) and the PEST sequence of ornithine decarboxylase, as reported previously[12]. The transfer plasmid pLV-TRE-EGFP.eTeNT.PEST was based the pFUGW[23] (a gift from D. Baltimore) and constructed by swapping the ubiquitin promoter-EGFP sequence with the tetracycline responsive element (TRE) of the pTRE-Tight vector (Clontech) and EGFP.eTeNT.PEST. For the control, the transfer plasmid pLV-TRE-EGFP.PEST was constructed by removing the eTeNT sequence from pLV-TRE-EGFP.eTeNT.PEST. The HiRet vector encoding EGFP.eTeNT or EGFP downstream of the TRE promoter (termed HiRet-TRE-EGFP.eTeNT or HiRet-TRE-EGFP) was prepared as described previously[18]. HEK293T cells were transfected with transfer, envelope and packaging plasmids by the calcium phosphate precipitation method. Viral vector particles were pelleted by centrifugation at 6,000*g* for 16–18 h and resuspended in phosphate-buffered saline (PBS). The particles were then applied to a Sepharose Q FF ion-exchange column (GE Healthcare) in PBS and eluted with a linear 0.0–1.5 M NaCl gradient. The fractions were monitored at absorbance of 260 or 280 nm. The peak fractions containing the particles were collected and concentrated by centrifugation through a Vivaspin filter (Vivascience). Functional titre (transduction unit) was measured by flow cytometry (FACSCalibur, Becton Dickinson). To determine the RNA titre, viral RNA in vector preparations was isolated with a NucleoSpin RNA Virus Kit (Clontech), and the copy number of the RNA genome was determined by using a Lenti-X qRT–PCR Titration Kit (Clontech). Polymerase chain reaction (PCR) amplification was performed on duplicate samples by using a StepOne Real-time PCR System (Life Technologies Corporation) under the following conditions: one cycle of 95 °C for 3 min; and 40 cycles of 95 °C for 15 s and 54 °C for 1 min. These lentiviral vectors were used within 2 weeks of their preparation.

The rtTA variant rtTAV16 was generated by introducing the V9I, G12S, F67S, F86Y, R171K and A209T mutations into rtTA2S-M2 of the pTet-On advanced vector (Clontech), as reported previously[14]. Plasmid pAAV2-CMV-rtTAV16 is based on pAAV-MCS (Agilent Technologies), constructed by inserting the CMV sequence of the pTet-On advanced vector, rtTAV16, the woodchuck hepatitis virus post-transcriptional regulatory element (WPRE) sequence of pFUGW, and the SV40 polyadenylation signal (SV40pA) of the pCMV-script vector (Agilent Technologies) into the MCS. The AAV vector for *in vivo* injection was produced as described previously[24].

To prevent adhesion of the AAV vector to the glass micropipettes, 0.001% Pluronic-F68 Solution (Sigma-Aldrich) was added to the vector solution. Because it was reported that the titre deteriorated by about 10% in 1 month in this stock condition[25], the vector solution was divided into small aliquots (each contained 10 μl of the vector solution) before being stored at −80 °C to reduce the number of freeze–thaw cycles. The vector solutions were used within 5 months of their preparation.

The development of the highly efficient Tet-on transactivator, rtTAV16, enabled the sharp onset of the effect of eTeNT transcription within 2 days, as revealed in this study. The propriospinal (PN) blockade seemed to have occurred earlier than the compensatory process, which enabled us to observe the behavioural effects. The Tet-off system, which is commonly used as a highly sensitive inducible system, requires 2 to 3 weeks to be effective[26]. Therefore, if we used the Tet-off system, the compensatory process might have occurred in parallel to the gradual initiation of the transmission block and we would not have been able to observe the behavioural effect.

Injection of vectors. Anaesthesia was induced by intramuscular injections of ketamine (1 mg kg^{-1}) (Daiichi Sankyo) and xylazine (1 mg kg^{-1}) (Bayer Health Care), then by pre-medication with dexamethasone (1 mg) (Merck Sharp and Dohme), atropine (0.5 mg) (Mitsubishi Tanabe Pharma) and gentamicin (10 mg) (Merck Sharp and Dohme). Under deep anaesthesia with isoflurane (1–2%) inhalation (Abbott Laboratories), the head of the monkey was fixed to the stereotaxic apparatus and surgery was carried out on the cervical spine from the dorsal approach. During surgery, mannitol (20%, w/v) was supplemented up to a total volume of 40 ml. Heart rate, O_2 saturation, partial pressure of CO_2 and body temperature were always monitored. In the case of the injections of HiRet-TRE-EGFP.eTeNT (titre, 3.9–7.5 × 10^{11} copies per ml) (or HiRet-TRE-EGFP; titre, 5.0 × 10^{11} copies per ml), laminectomy was performed on the C4–C7 vertebrae to expose the C6–T1 segments on the left side (right side only in the case of monkey S). A glass micropipette (with a tip diameter of 100 μm) was filled with the vector solution. The injections were intended to be made at the point in the dorsal column at 0.5–1.0 mm medial to the dorsal root entry zone to avoid the vessels on the surface of the spinal cord. The pipette was inclined by 10 degrees towards the lateral side. A small hole was made on the dura with a 20-gauge injection needle and the pipette approached the spinal cord through the hole. The tip of the pipette was initially set at 4.5 mm from the dorsal surface of the spinal cord and then pulled up to a depth of 4 mm and fixed. Then 0.5 μl vector solution was injected for 5 min under the control of a microinfusion pump (Eicom) and after termination of the injection, the pipette was fixed at the same position for another 5 min and then pulled out. In the case of the HiRet-TRE-EGFP.eTeNT (or HiRet-TRE-EGFP) injections, 16–19 injections were made into the ventral horn at 1-mm intervals throughout the C6–T1 segments in four monkeys (H, K, B and N). In one monkey (S), HiRet-TRE-EGFP was injected in the same way, as a control. After injection, the dura was covered with Sponzel (Astellas Pharma), and muscles and skins were closed by suturing. After the surgery, diclofenac sodium (Voltaren, Novartis) was routinely applied to the anus for analgesia.

Seven to ten days after the HiRet-TRE-EGFP.eTeNT or HiRet-TRE-EGFP injection, AAV2-CMV-rtTAV16 (titre, 2.0 × 10^{13} particles per ml) was injected into the intermediate zone of the caudal C2 to rostral C5 segments. The surgical procedures were similar to the previous surgery, except for the level of laminectomy (caudal part of the C1 vertebra, and C2 and C3 vertebrae). The glass micropipette containing AAV2-CMV-rtTAV16 was inserted into the spinal cord perpendicularly with the entrance at 500 μm medial to the dorsal root entry zone. The tip of the pipette was initially inserted to a depth of 4 mm from the dorsal surface of the spinal cord and then lifted to a depth of 3.5 mm before the AAV2-CMV-rtTAV16 was injected (0.5 μl for each site, 5 min for the injection and another 5 min leaving the pipette in position). Injections were made at 1 mm intervals throughout the C2–C5 segments. A total of 8–13 injections were made.

Administration of doxycycline. Doxycycline administration was initiated at 1 to 2 months after the vector injections (Fig. 1c and Supplementary Table 1). Doxycycline was dissolved in 3% sucrose water and administered at a dose of 5–15 mg kg^{-1} per day orally to the monkey every morning. Each period of administration lasted for 6 to 9 days. For measuring the blood doxycycline concentration, a blood sample (2 ml) was taken in the evening immediately before, during and after doxycycline administration. Doxycycline concentration was measured with high-performance liquid chromatography (LC-MS/MS system 6400, Agilent Technologies; an analysis service was provided by Towa Environmental Science) as described previously[27].

Behavioural tests. The five monkeys were trained to sit in their home cage and reach for pieces of sweet potato or carrot (7 × 7 × 7 mm^3) through the window on the acrylic front panel of the cage. A vertical slit of 1 cm width was set in front of the monkey and the food piece was presented between the slit (Fig. 2a, c), so that the monkey could only use its index finger and thumb to pick up the food. The distance between the food piece and entrance edge of the slit was kept constant for each monkey throughout the experiments. Each session consisted of 30–100 reach and grasp movements and were performed once or twice a day. The hand movements were video filmed from the side and the movement parameters were analysed off-line. We measured the number of error trials in each session. We defined the three following types of errors. A 'precision grip error' was judged by the same criteria as those used in a previous report[8,9] (Fig. 2a, b and Supplementary Movie 1). If the finger touched but did not pass the edge of slit and stayed there for more than 66 ms (2 video frames), we judged it to be a 'slit-hit error' (Fig. 2c, d and

Supplementary Movie 2). If both fingers touched the food but the monkey released it and tried to pick it up again, we judged it as a 'wandering error' (Supplementary Movie 3). The error rate was calculated as the number of error trials divided by the total number of trials in the session. For the baseline, we calculated the average and s.d. of the error rates in the sessions performed between days −4 and 0 from the start of doxycycline administration. Day 0 was included in the baseline period, because doxycycline administration was performed just after the behavioural test session in the morning. Filled red circles in Fig. 2e indicate that the error rate in the session was higher than the average plus 2.58 s.d. (representing the 99% level of the normal distribution) of the baseline period. Movement time was defined as the interval between the moment when any finger touched or passed the edge of the slit, and the moment when all the fingers exited from the edge of slit. Filled blue circles in Fig. 2e indicate that the movement times in the session were significantly longer than those during the baseline period (days −4 to 0) (two-tailed *t*-test, $P < 0.001$). The trials in which the monkey dropped the food piece were excluded from the analysis of the movement time.

Electrophysiological experiments. On the last day of the final period of doxycycline administration, synaptic transmission through the PNs was investigated with electrophysiological experiments under anaesthesia. The basic experimental design has been described previously[5–7,10].

The animals were first anaesthetized with ketamine (1 mg kg^{-1}) and xylazine (1 mg kg^{-1}) and after the tracheotomy, isoflurane (1–2%) inhalation was used for anaesthesia throughout surgery. After surgery, anaesthesia was changed to α-chloralose (75–150 mg kg^{-1}) (Sigma-Aldrich). Blood pressure was maintained at ~100 mm Hg and with a partial pressure of CO_2 at ~4%. The depth of anaesthesia was continuously monitored by checking the stable blood pressure and lack of a pupillary reflex. A drip of Ringer's solution with glucose and doxycycline was given during the entire experiment and the urinary bladder was emptied regularly. Dexamethasone (1 mg) and gentamicin (10 mg) were given just after anaesthesia. Atropine was given at intervals of 4 to 5 h. The animals were paralysed with pancuronium bromide (1 ml, 0.2 mg ml^{-1}) (Merck Sharp and Dohme) given at 30-min intervals, and artificially ventilated with a pump. A pneumothorax was made just before electrophysiological recordings.

A craniotomy was made to expose the posterior part of the cerebellum and the caudal brainstem in order to place the pyramidal electrode. The electrode position was calibrated at the obex (65° from the vertical line) and placed ~2.5 mm rostrally, 1.25 mm laterally and at a depth of ~5.0 mm from the dorsal surface of the brainstem. The threshold for eliciting the descending pyramidal volley was ~5 μA. Monopolar cathodal pulses (0.1 ms duration) were applied using tungsten electrodes with an impedance of ~50–100 kΩ and a tip diameter of 10 μm. The stimulating electrode in the lateral reticular nucleus (LRN) was set 2 mm caudal to the obex, 3.5 mm lateral from the midline, and at 5.5 mm from the surface of the brainstem, which corresponded to the mediodorsal edge of the LRN[6]. A laminectomy was made at the C2–T1 segments. The deep radial nerve was stimulated with needle electrodes inserted through the skin. Intracellular recordings from antidromically identified forelimb motor neurons (and unidentified motor neurons) in the lateral motor nuclei of the C6–T1 segments were performed as described previously[5–7,10], and field potential recordings from the deep radial motor nuclei were made using glass microelectrodes filled with 2 M potassium citrate (impedance 2–5 MΩ). The location of the deep radial motor nucleus was identified by the criterion that the amplitude of antidromic field potentials from the deep radial nerve was larger than 0.2 mV. The depths of recordings from the dorsal surface of the spinal cord ranged from 2.8 to 4.1 mm. Individual recording sites were separated more than 200 μm from each other and randomly sampled. The cord dorsum potential (CDP) was recorded using a silver ball electrode put on the dorsal surface of the spinal cord in proximity to the microelectrode penetration site to determine the timing of the arrival of the corticospinal tract (CST) volley. Segmental latencies of synaptic responses, that is, the latencies following the positive peak of the direct CST volley on the CDP, indicate the time spent in the same segment after the arrival of the fastest conducting fibres. These times were measured to identify of the synaptic linkage of the evoked responses. Strychnine (0.1 mg kg^{-1}, given repeatedly to maintain the excitability level) (Sigma-Aldrich) was injected intravenously at the early stage of the experiments to reduce glycinergic inhibition, by which the disynaptic excitation of motor neurons from the CST[5,6] was unmasked. During the experiment, after recording the monosynaptic corticomotoneuronal effects, the CST was lesioned at the C5 or C2 level by mechanical transection of the dorsolateral funiculus (DLF) with fine forceps to localize the interneurons mediating the disynaptic excitation from the CST, either on the segmental interneurons (sINs), PNs or reticulospinal neurons (RSNs). Completeness of the lesion was assessed by measuring the CDP responses to contralateral medullary pyramid stimulation recorded caudally to the lesion.

Histological assessment. At the end of the experiments, the monkeys were deeply anaesthetized with intravenous injection of sodium pentobarbital (80–100 mg kg^{-1}) (Hospira) and transcardially perfused with 0.05 M PBS and then 4% paraformaldehyde in 0.1 M phosphate buffer (pH 7.4). The brainstem and spinal cord were cryoprotected and sectioned at a thickness of 40 μm using a cryostat. Spinal cord tissues were examined for the distribution of EGFP-positive neurons with anti-GFP immunohistochemistry and the distribution of AAV2-CMV-rtTAV16-infected neurons with *in situ* hybridization to detect the rtTA sequence.

Anti-GFP immunohistochemistry. After observation and photographing of GFP fluorescence using fluorescent microscopes (Axioplan 2, Zeiss; and BIOREVO, BZ-9000, Keyence), the sections were immunohistochemically stained with a GFP antibody[28]. Every three to five sections were dipped in PBS with 0.3% Titon-X (PBST) containing 5% skimmed milk at room temperature and then with a rabbit anti-GFP antibody (1:2,000; Life Technologies) in PBST for 16 h at 4 °C. The sections were washed in PBST and incubated in biotinylated goat anti-rabbit IgG (1:200; Vector Laboratories) and then ABC-Elite (1:200; Vector laboratories) and visualized with diaminobenzidine (1:10,000; Wako) containing 1% Nickel sodium ammonium and 0.0003% H_2O_2 in Tris-buffered saline. The sections were counterstained with Neutral Red.

The number of GFP-positive cells was counted in every fifth section (each section was 40 μm thick) using a BZ-51 microscope (Olympus). The number of cells in two adjacent sections was averaged to estimate the number of PNs within every 400 μm of the rostrocaudal extent.

***In situ* hybridization to visualize rtTAV16.** Infection of AAV2-CMV-rtTAV16 carrying rtTAV16 was examined by *in situ* hybridization. This method has been described elsewhere[29–31]. Briefly, free-floating sections (40 μm) were treated with proteinase K (5 μg ml^{-1}) and hybridized with the rtTA antisense probe at 60 °C overnight. After washing, the hybridized probe was detected using an alkaline-phosphatase-conjugated anti-digoxigenin antibody followed by nitro blue tetrazolium (NBT) and 5-bromo-4-chloro-3-indolyl phosphate (BCIP) colorization. The plasmid for the probe was constructed by cloning the EcoRI- and BamHI-digested fragment of the lentiviral plasmid, STB[32] into pBlueScriptII. This plasmid was linearized by EcoRI and used for digoxigenin labelling of the antisense RNA probe. This probe detected the expression of both Tet-off and Tet-on transactivators including rtTAV16. The detailed protocol for *in situ* hybridization is also available on the web (http://www.nibb.ac.jp/brish/indexE.html). The number of rtTA-positive cells was counted in every 15th section throughout the AAV2 vector injected sites.

23. Lois, C., Hong, E. J., Pease, S., Brown, E. J. & Baltimore, D. Germline transmission and tissue-specific expression of transgenes delivered by lentiviral vectors. *Science* **295,** 868–872 (2002).
24. Kaneda, K. *et al.* Selective optical control of synaptic transmission in the subcortical visual pathway by activation of viral vector-expressed halorhodopsin. *PLoS ONE* **6,** e18452 (2011).
25. Croyle, M. A., Cheng, X. & Wilson, J. M. Development of formulations that enhance physical stability of viral vectors for gene therapy. *Gene Ther.* **8,** 1281–1290 (2001).
26. Nakashiba, T., Young, J. Z., McHugh, T. J., Buhl, D. L. & Tonegawa, S. Transgenic inhibition of synaptic transmission reveals role of CA3 output in hippocampal learning. *Science* **319,** 1260–1264 (2008).
27. Böcker, R. Analysis and quantitation of a metabolite of doxycycline in mice, rats, and humans by high-performance liquid chromatography. *J. Chromatogr.* **274,** 255–262 (1983).
28. Kato, S. *et al.* Efficient gene transfer via retrograde transport in rodent and primate brains using a human immunodeficiency virus type 1-based vector pseudotyped with rabies virus glycoprotein. *Hum. Gene Ther.* **18,** 1141–1151 (2007).
29. Komatsu, Y., Watakabe, A., Hashikawa, T., Tochitani, S. & Yamamori, T. Retinol-binding protein gene is highly expressed in higher-order association areas of the primate neocortex. *Cereb. Cortex* **15,** 96–108 (2005).
30. Watakabe, A., Komatsu, Y., Ohsawa, S. & Yamamori, T. Fluorescent in situ hybridization technique for cell type identification and characterization in the central nervous system. *Methods* **52,** 367–374 (2010).
31. Watakabe, A. *et al.* Comparative analysis of layer-specific genes in Mammalian neocortex. *Cereb. Cortex* **17,** 1918–1933 (2007).
32. Hioki, H. *et al.* High-level transgene expression in neurons by lentivirus with Tet-Off system. *Neurosci. Res.* **63,** 149–154 (2009).